CHAPTER IV
VERTICAL TWO-PHASE FLOW REGIME AND PRESSURE GRADIENT UNDER THE INFLUENCE OF SDS SURFACTANT

Tanabordee Duangprasert[a], Anuvat Sirivat[a,*],

Kitipat Siemanond[a],*, James O. Wilkes[b]

[a]*The Petroleum and Petrochemical College, Chulalongkorn University, Soi Chula12, Phayathai Road, Pathumwan, Bangkok 10330, THAILAND*

[b]*Department of Chemical Engineer, The University of Michigan, Ann Arbor, U.S.A*

4.1 Abstract

Two-phase gas/liquid flows in vertical pipes have been systematically investigated because of their importance in many industrial processes operating in the two-phase flow regimes. There are four principle flow regimes which occur successively at ever-increasing gas flow rates: the bubble, the slug, the annular, and the mist flow regimes. In this research, the flow regimes and their pressure gradients were be investigated at a fixed temperature of 30°C. Water and SDS solution (1 CMC) were used as the working fluids. In particular, we focused our work on the influence of surfactant addition on the flow regimes and the corresponding pressure gradients of the two-phase flow in a vertical pipe. An experiment was carried out in a vertical transparent tube with 0.019 m inner diameter and 3 m in length, and pressure gradients were measured by the pressure taps connected to a U-tube manometer. For both solutions, at a fixed Re_{water} or $Re_{SDS\ solution}$ with increasing Re_{air}, the pressure gradients decreased from the bubble flow regime to the churn flow regime. In the annular to mist flow regimes, the pressure gradients increased with increasing Re_{air}. In the slug and the slug-churn flow regimes, the pressures gradients of the SDS solutions decreased with increasing SDS concentrations, relative to that of water. At

a fixed Re_{water} or $Re_{SDS\ solution}$ with increasing Re_{air}, the bubble height increased but the bubble width seems to be constant. At a fixed Re_{air}, the bubble velocity increased with increasing Re_{water} or $Re_{SDS\ solution}$. Finally, the experimentally measured pressure gradient values were compared with the theoretical values and they were in good agreement.

(Key-words: vertical two-phase flow flow, surface tension, pressure gradient, bubble size, bubble velocity, superficial gas /liquid velocity and Reynolds number)

*Corresponding author: email anuvat.s@chula.ac.th, Ph: 662 218 4131, Fax: 662 611 7221

*Corresponding author: email kitipat.s@chula.ac.th Ph: 662 218 4136, Fax: 662 215 4459

*The Petroleum and Petrochemical College, Chulalongkorn University, Bangkok, Thailand, 10330

4.2 Introduction

Two-phase gas and liquid flows in vertical pipe have been investigated in details because of their importance in many industrial processes that utilize pipe and equipment operating under in two-phase flows. The vertical two-phase flow regimes can strongly influence to the pressure drop or the energy loss, the holdup, the system stability, and the exchange rates of heat, mass, and momentum. There are five flow regimes which occur at ever-increasing the gas flow rate: (1) the bubble flow; (2) the slug flow; (3) the churn flow; (4) the annular flow; and (5) the mist flow. Flow regimes depending on many factors, the individual magnitudes of the liquid and gas flow rate: the physical properties such as density, viscosity, and surface tension [1].

Bubble flow regime is characterized by the gas phase dispersed throughout the liquid phase along with bubbles of various sizes. Typically, the bubbles are small compared with the diameter of the pipe: their shapes are not generally influenced by the presence of the pipe wall [2]. The bubble-to-slug transition is due to collisions between many small bubbles, with a fraction of these collisions resulting in coalescence, ultimately leading to bubbles which are compare in size to the pipe diameter, and hence the slug flow [3]. In the slug flow regime, most of the gas is located in large bullet-shaped bubbles, the so-called Taylor bubbles, which occupy most of the pipe cross section. The liquid between Taylor bubble and pipe wall flows around as a thin film and Taylor bubbles are separated by liquid slugs which may contain small bubbles [4]. At higher gas flow rates, a transition from the slug flow regime to the churn flow occurs. In the churn flow regime, the continuity of the liquid phase in the slug between successive Taylor bubbles is destroyed by the gas phase, and when this occurs happens the liquid slug falls. The distinguishing feature of churn flow is an oscillatory up and down motion of the liquid slugs as well as the liquid film on the pipe wall [5].

The annular and mist flow regimes are commonly encountered in the flow of gas-liquid mixtures at very high gas flow rates and high gas-liquid ratio [6]. The annular flow regime is characterized by the liquid phase traveling as a film on the channel pipe walls and the gas phase flowing up through the center. Part of the liquid can be carried as droplets in the central gas core. Because the velocity of the

gas phase is high, the thickness of liquid film on the pipe wall decreases and the droplets are torn from the liquid film and entrained in the central gas core.

Detailed characteristics and measuring methodology for setting the flow regime of a two-phase liquid and gas flow can be found amongst many previous work of Nicklin *et al.* [2], Davies and Taylor [7], Wallis [8], Martinelli and Lockhart [9], Wilkes [1], and Sylvester [10].

Furukawa and Fukano [11] investigated the effect of liquid viscosity on the flow pattern. They assumed that the change in the density and the surface tension were negligibly small while the viscosity changed upto about 15 times relative to that of water. They found that the flow pattern transitions strongly depend on the liquid viscosity. McNeil and Stuart [12] studied the effect of a highly viscous liquid phase by using water and glycerine solution to produce nominal liquid viscosity of 1, 50, 200, and 500 mPa.s. They found that the very large pressure drops occurring with the high viscosity fluids gave rise to substantial velocity and density variations within the test section. Dziubinski et al. [13] investigated the flow patterns of a two-phase flow of a gas and a non-Newtonian liquid in a vertical pipe. Multi-phase mixtures 5% carboxymethylcellulose (CMC) aqueous solutions and suspensions of 2-17.8 wt.% spherical glass particles in CMC solutions were used as the continuous phase. They found that the non-Newtonian features of liquid had a negligible effect on the type of the two-phase flow structure and the most distinct feature appeared to be the apparent velocities of liquid and gas flow. Malayeri et al. [14] analyzed and characterized the dominant variables that influence the void fraction at higher temperature. They found that void fraction increased only marginally from 20 to 60 °C, but then increased sharply in particular near the boiling point.

We are not aware of any investigation on the effect of liquid surface tension on the flow regimes and the pressure gradients. The objectives of our work are to investigate the effect of surfactant (surface tension) on the flow regimes, the corresponding pressure gradients, the bubble size and the bubble velocity. The pressure gradients from the experiment are compared with those calculated from the theories.

4.3 Experimental Apparatus

Air, water, and SDS ($C_{12}H_{25}NaO_4S$) solutions at 0.5, 1, and 2 CMC (Riedel-de Haen, 90% purity) were used as the working fluids. The main components of the system consisted of the vertical test section, an air supply, and instrumentation. The pipe with 1.9 cm inside diameter and the length of 300 cm made from transparent acrylic glass to permit visual observation of the flow patterns was used as the test section. The scheme of the experimental set up is shown in Figure 1. At the bottom of the main column there is an inlet for the compressed air from a compressor (Taiwan, Fu Sheng HTA-100H) and flow rates were measured by a calibrated air-rotameter (Cole-Parmer, A-32466-68, U.S.A.). Liquid was pumped from the storage tank through a rotameter and mixed with air at the bottom of the main column. The flow rates of the liquid were measured by a calibrated liquid-rotameter (Cole-Parmer, U.S.A, A-32461-42). Liquid flowed upward through the main column together with air and then flowed back to the storage tank. Two static pressure tabs were installed at two axially locations with the spacing of 0.4 m and connected with a custom made manometer which was used to measure the pressure drops along the test section. Physical properties of liquids used in the experiment are list in Table 1.

Experiments were conducted by varying air and liquid flow rates. The air flow rate was increased by small increments while the liquid (pure water or SDS solutions) flow rate was kept constant. The experimental conditions were as follows: superficial air velocity j_{air}: 0.0026~58.81 m/s, superficial water velocity j_{water}: 0~0.123 m/s, superficial SDS solution (1 CMC) velocity $j_{SDS\ solution}$: 0~0.1359 m/s respectively. Air and liquid temperatures varied between 31~32°C. The system was allowed to approach the steady condition before any data was taken. The pressure drops across the test section were detected at different flow rates of air and liquid. The flow regimes were observed and identified by visual observation: a video camera (Panasonic, NV-M3000) and software program (Win DVD). Bubble size, slug size and void fraction of Taylor bubble were identified and measured by a software program (Scion Image). Bubble velocity was measured by timing bubbles traveling past at known distances.

4.4 Results and Discussion

4.4.1 Visual Observations of the Flow Regime by Still Photographs

When the superficial air velocity, j_{air} was low, the bubble flow was observed. The flow pattern basically changed from the bubble flow to the mist flow with increasing j_G at a fixed j_L value. As the superficial air velocity, $j_{air,}$ was increased, the flow regime changed from the bubble to slug, the churn, the annular, and the mist flow regimes, respectively. All the boundaries between the bubble-slug, the slug, the slug-churn, the churn, the annular, and the mist regimes were identified by direct visual observation of the flow patterns as well as by observations through the digital camera and the video camera. The critical Reynolds number of air $(Re_{air})_{critical}$ for each flow regime was identified and the boundaries of the flow patterns observed; they are listed in Table 2. For same j_L values, the SDS solution (1 CMC) boundaries of the bubble, the bubble-slug, and the slug flow regimes shifted to lower critical Reynolds number of air. For the churn, the annular, and the mist flow regimes, the boundaries did not change because the air Reynolds numbers, (Re_{air}), were high and the flow was highly turbulent, and consequently the effects of viscosity and surface tension were negligible.

4.4.2 Effect of $Re_{SDS\ solution}$ at 1 CMC on Pressure Gradient (dp/dz)

Figures 2(a), 2(b), and 2(c) show the comparison of the measured pressure gradients, $(dp/dz)_{exp}$, with air Reynolds numbers, Re_{air} for pure water and the SDS solution (1 CMC) at the same liquid Reynolds numbers. As we increased Re_{air}, the pressure gradients decreased steadily from the bubble flow regime to the slug-churn flow regime for both pure water and the SDS solution (1 CMC). But in the churn flow regime, the pressure gradients increased slightly and decreased again. Finally, from the annular flow to the mist flow, the pressure gradients increased with increasing air Reynolds numbers for both the pure water and the SDS solution (1 CMC). At the same liquid Reynolds numbers, the pressure gradients, $(dp/dz)_{exp}$, of the SDS solution (1 CMC) seemed to be equal to the pressure gradients, $(dp/dz)_{exp}$, of the pure water in the bubble and bubble-slug flow regimes. The pressure gradients, $(dp/dz)_{exp}$, of the SDS solution (1 CMC) were lower than the pressure gradients,

$(dp/dz)_{exp}$, of the pure water in the slug flow to the slug-churn flow regime and they were nearly equal to each other again in the churn flow regime. In the annular and the mist flow regimes at low liquid Reynolds numbers, the pressure gradients, $(dp/dz)_{exp}$, of the SDS solution (1 CMC) was higher than the pressure gradients, $(dp/dz)_{exp}$, of the pure water. In the same regimes and at high liquid Reynolds numbers, the pressure gradients, $(dp/dz)_{exp}$, of the SDS solution (1 CMC) was lower than the pressure gradients, $(dp/dz)_{exp}$, of the pure water.

In Figure 2(a), the liquid flow rates were zero; therefore we could only obtain data up to the slug flow regime. In Figures 2(b) to 2(c), we show the measured pressure gradients from the bubble to the mist flow regimes. Fluctuations in the pressure gradients, $(dp/dz)_{exp}$, occurred in every flow regimes but they were less severe in the bubble, the annular, and the mist flow regimes. Fluctuations of pressure gradients, $(dp/dz)_{exp}$, were less in the SDS solution (1 CMC) than those of the pure water. The highest fluctuations occurred in the slug-churn transition as the Taylor bubbles in slug flow started to break down into an unstable pattern in which there was a churning or oscillatory motion of liquid.

4.4.3 Effect of Surfactant Concentration on Pressure Gradient (dp/dz)

Figure 3 shows the comparison of the measured pressure gradients, $(dp/dz)_{exp}$, with air Reynolds numbers, Re_{air}, at various SDS concentrations at the same liquid Reynolds numbers. For pure water and the SDS solution at 1 CMC, we measured the pressure gradient from the bubble to the mist flow regime. For the SDS solution at 0.5 and 2 CMC, we measured the pressure gradients from the bubble-slug regime to the churn flow regime. At the same liquid Reynolds numbers, the pressure gradients, $(dp/dz)_{exp}$, of the SDS solutions at 0.5, 1 and 2 CMC are nearly equal to each others, but they are certainly lower than the pressure gradient (dp/dz) of pure water in the slug and the slug-churn flow regimes. The pressure gradients of all fluids tested are nearly equal to each other again in the churn flow regime. We may note the surface tension for all of SDS solutions are nearly equal to each other but they are lower than that of pure water due to the presence of surfactant, as shown in Table 1. It is possible that the smaller pressure gradients of SDS solutions arise from the turbulent drag reduction effect.

4.4.4 Comparison Between Theoretical and Measured Pressure Gradients, (dp/dz)

Figures 4(a), 4(b), and 4(c) show the comparison of the pressure gradients obtained from experiments $(dp/dz)_{exp}$ and the predicted $(dp/dz)_{cal}$ values from the theories. In Figures 4(a) to 4(c), we compared the predicted values and the measured values of the pressure gradient in the bubble flow, the slug flow, the annular flow and the mist flow regimes.

Bubble Flow Regime

The pressure gradient can be calculated fairly accurately by considering only the hydrostatic effect. For the relatively low liquid velocities likely to be encountered in the bubble-flow regime, friction is negligible. The predicted pressure gradients, $(dp/dz)_{cal}$ for the bubble flow regime are proposed by Nicklin, Wilkes, and Davidson [2] as in the following equation:

$$\left(-\frac{dp}{dz}\right) = \rho_L \, g \, (1-\varepsilon) \tag{1}$$

where ρ_L = liquid density (kg/m^3), g = gravitational acceleration constant (m/s^2), and ε = void fraction of air. This equation implies that the predicted $(dp/dz)_{cal}$ can be determined if the liquid density, ρ_L, and void fraction of air, ε, were known. The void fraction of air, ε, was also proposed by Nicklin, Wilkes, and Davidson [2] from the following equation if Q_G and Q_L are known.

$$\text{Void fraction} = \varepsilon = \frac{Q_G}{(Q_G + Q_L) + u_b \, A} \tag{2}$$

where Q_G = volumetric flow rate of gas (l/min), Q_L = volumetric flow rate of liquid (l/min), A = cross-sectional area of the pipe (m^2), (dp/dz) = pressure gradient (kPa/m), u_b = bubble rise velocity in a stagnant liquid (m/s). The bubble velocity, u_b rising into a stagnant liquid was proposed by Davies and Taylor [7].

$$\text{Bubble velocity} = u_b = 1.00\sqrt{g \, R_b} \tag{3}$$

where g = gravitational acceleration constant (m/s^2), R_b = radius of a sphere that has the same volume as the spherical-cap bubble (m).

Slug Flow Regime

The predicted pressure gradient, $(dp/dz)_{cal}$ for the slug flow regime was proposed by Nicklin, Wilkes, and Davidson as in the following equation [2]:

$$\left(-\frac{dp}{dz}\right) = (1-\varepsilon)\left[\rho_L g + \left(\frac{dp}{dz}\right)_{sp}\right] \tag{4}$$

Single-phase frictional pressure gradient for the liquid only is:

$$\left(-\frac{dp}{dz}\right)_{sp} = \frac{2 f_F \rho_L \overline{u_L}^2}{D} \tag{5}$$

The single-phase pressure gradients can be calculated with the friction factors, $f_F = 16/\mathrm{Re}$ for laminar flow (Re < 2000), and $f_F = 0.0790\,\mathrm{Re}^{-1/4}$ for turbulent flow (Re > 4000). The Reynolds number of the liquid, $\mathrm{Re}_L = \left(\overline{u_L}\, D\right)/\nu_L$ and mean upward liquid velocity, $\overline{u_L}$ can be calculated from, $\overline{u_l} = \left(Q_G + Q_L\right)/A$. The calculation of the void fraction of air, ε , can be calculated from the following equation by Nicklin, Wilkes, and Davidson [2]:

$$\text{Void fraction} = \varepsilon = \frac{Q_G}{1.2(Q_G + Q_L) + u_b A} \tag{6}$$

where Q_G = volumetric flow rate of gas (l/min), Q_L = volumetric flow rate of liquid (l/min), A = cross-sectional area of the pipe (m^2), u_b = bubble rise velocity in a stagnant liquid (m/s).

The bubble rise velocity, u_b rising into a stagnant liquid was proposed by Davies and Taylor [7] as in the the following equation:

$$\text{Bubble rise velocity} = u_b = c\sqrt{g\,D} \tag{7}$$

where g = gravitational acceleration constant (m/s^2), D = diameter of the pipe (m). The experiments indicate that the constant "c" was 0.35 [7].

Another theory for the predicted pressure gradient, $(dp/dz)_{cal}$ for the slug flow regime was proposed by Sylvester [10]. Sylvester (1987) showed the mechanistic model for calculating the pressure gradient for slug flow. The mechanistic model for vertical slug flow was formulated based on the assumption that the flow is fully developed and stable. This assumption requires that a liquid slug and the Taylor bubble rise steadily without any relative velocity between them. The model was developed in term of a slug unit consisting of a slug unit and a Taylor bubble along with its surrounding liquid.

The total pressure drop in the slug unit consists of three components

$$(\Delta P)_T = (\Delta P)_A + (\Delta P)_H + (\Delta P)_F \tag{8}$$

where $(\Delta P)_T$ is the total pressure drop in the slug unit, $(\Delta P)_A$ is the acceleration pressure drop, $(\Delta P)_H$ is the hydrostatic pressure drop, and $(\Delta P)_F$ is the frictional pressure drop.

The acceleration pressure drop is taken into account required to reverse the direction of and to accelerate the liquid film falling around the Taylor bubble to the velocity U_{LLS}. This pressure drop can be written as

$$(\Delta P)_A = \rho_L(U_{LTB} + U_{TB})(1-\alpha_{TB})(U_{LTB} + U_{TB} + U_{LLS}) \tag{9}$$

where

$$U_{LTB} = 9.916\left[gD\left(1-\sqrt{\alpha_{TB}}\right)\right]^{1/2} \tag{10}$$

$$U_{TB} = 1.2(U_{SG} + U_{SL}) + 0.35\left[\frac{gD(\rho_L - \rho_G)}{\rho_L}\right]^{1/2} \tag{11}$$

The hydrostatic pressure drop of the slug unit can be written in the form

$$(\Delta P)_H = \rho_L(1-\alpha_{LS})gL_{LS} \tag{12}$$

where

$$\alpha_{LS} = \frac{U_{SG}}{C_2 + C_3(U_{SG} + U_{SL})} \tag{13}$$

In equation (13), $C_2 = 0.425$ and $C_3 = 2.65$ were chosen[15]. It must be emphasized that although the form of equation (13) is theoretically sound, the

coefficients were determined from a best least squares fit of Fernandes experiment data [15].

The frictional pressure drop of a slug unit can be written as

$$(\Delta P)_F = \frac{L_{LS}}{2D}\left[\frac{\rho_G \beta f_{TB} U_{TB}^2}{(1-\beta)\left[1-(1-\alpha_{TB}^{1/2}\right]} + U_{LLS}^2 \rho_L (1-\alpha_{LS}) f_{LS} (1-\beta)\right] \tag{14}$$

where

$$\beta = L_{TB}/L_{SU} \tag{15}$$

and f_{TB} is friction factor associated with the Taylor bubble. If it is assumed that the falling rough surface to the Taylor bubble, the Taylor bubble friction factor may be written as

$$f_{TB} = \frac{1}{\left[-2.0\log\left\{\frac{\left(1-\alpha_{TB}^{1/2}\right)}{7.4}\right\}\right]^2} \tag{16}$$

f_{LS} is the friction factor associated with the liquid slug which in general depends upon the Reynolds number of the liquid slug , Re_{LS}, and the pipe roughness. This dependency can be expressed as

$$f_{LS} = f_{LS}(\mathrm{Re}_{LS}, \varepsilon / D) \tag{17}$$

where ε is the pipe roughness, and

$$\mathrm{Re}_{LS} = \frac{\rho_L (1-\alpha_{LS}) U_{LLS} D}{\mu_{LS}} \tag{18}$$

Since $\mu_L >> \mu_G$ equation (12) may be simplified to

$$\mu_{LS} \cong \mu_L (1-\alpha_{LS}) \tag{19}$$

Equation (17) can be expressed explicitly using the Zigrang-Sylvester equation [15] which is an explicit representation of the Colebrook equation.

$$f_{LS} = \frac{1}{\left[-2.0\log\left\{\frac{\varepsilon/D}{3.7} - \left(\frac{5.02}{\mathrm{Re}_{LS}}\right)\log\left(\frac{\varepsilon/D}{3.7} + \frac{13}{\mathrm{Re}_{LS}}\right)\right\}\right]^2} \tag{20}$$

Substituting equations (9), (12) and (14) into equation (8) gives the total pressure drop for a slug unit.

$$(\Delta P)_T = \rho_L (U_{LTB} + U_{TB})(1-\alpha_{TB})(U_{LTB} + U_{TB} + U_{LLS}) + \rho_L (1-\alpha_{LS}) g L_{LS} + \frac{L_{LS}}{2D}\left[\frac{\rho_G \beta f_{TB} U_{TB}^2}{(1-\beta)\left[1-(1-\alpha_{TB}^{1/2}\right]} + U_{LLS}^2 \rho_L (1-\alpha_{LS}) f_{LS} (1-\beta)\right] \tag{21}$$

Annular and Mist Flow Regimes

The pressure gradients, $(-dp/dz)_{cal}$ for the annular and the mist flows were proposed by Wallis [8]; they used the Lockhart-Martinelli correlation [9] for the friction part of the pressure gradient, supplemented with appropriate gravitational terms. We now consider two parts for the pressure gradient calculation. First, consider just the flow of gas in the inner core. The momentum equation for the gas core was proposed by Wallis [8] as:

$$\left(\frac{dp}{dz}\right)_{tp} = \left(\frac{dp}{dz}\right)_g = -\frac{2 f_F \rho_g v_g^2}{D_g} - \rho_g g = \phi_g^2 \left(\frac{dp}{dz}\right)_{go} - \rho_g g \tag{22}$$

Second, the momentum equation for the entire flow was also proposed by Wallis [8]:

$$\left(\frac{dp}{dz}\right)_{tp} = \phi_l^2 \left(\frac{dp}{dz}\right)_{lo} - \left[\varepsilon \rho_g + (1-\varepsilon)\rho_l\right] g \tag{23}$$

Eliminating the two-phase pressure gradient between these two equations gives a single equation with three unknowns, ϕ_g^2 = the gas two-phase flow multiplier, ϕ_l^2 = the liquid two-phase flow multiplier, and ε = the void fraction of air.

In the Lockhart-Martinelli model [9], the gas two-phase flow multiplier ϕ_g is defined as:

$$\phi_g^2 = \frac{(dp/dz)_{tp}}{(dp/dz)_{go}} \tag{24}$$

where $(dp/dz)_{tp}$ is two-phase pressure gradient, and $(dp/dz)_{go}$ is the gas only pressure gradient. The Lockhart-Martinelli model [9] provides correlations for the multiplier based on the Martinelli parameter defined as:

$$X^2 = \frac{(dp/dz))_{lo}}{(dp/dz)_{go}} = \frac{\phi_g^2}{\phi_l^2} \tag{25}$$

where $(dp/dz)_{lo}$ is the pressure gradient of the liquid flowing alone in the tube. The correlations between X, ϕ_g and ε *is:*

$$\phi_g = \left(1 + X^{2/n}\right)^{n/2} \tag{26}$$

$$\varepsilon = \frac{1}{\left(1 + 0.0904\, X^{0.548}\right)^{2.82}} \tag{27}$$

where the exponent for two-phase correlation "n" based on the gas/liquid phase laminar or turbulent flow [1]. Finally, we put these correlations into a single equation with three unknowns, ϕ_g^2, X, and ε and obtain the general equation to find "X" for pure water and SDS solution (1 CMC). The Martinelli parameter "X" can be calculated from the single-phase pressure gradient using the standard friction factor approach. For pure water, "X" is defined as:

$$\left(1 + X^{2/3.61}\right)^{3.61}\left((dp/dz)_{go} - \frac{(dp/dz)_{lo}}{X^2}\right) = 9749\left(1 - \frac{1}{\left(1 + 0.0904 X^{0.548}\right)^{2.82}}\right) \tag{28}$$

We obtain this equation by equating the equations (22) and (23) and eliminating the two-phase pressure gradient to get a single equation with three unknowns, ϕ_g^2, ϕ_l^2 and ε. Finally, we replace ϕ_l^2 with Martinelli parameter "X" by

using equation (25), replace ϕ_g^2 with Martinelli parameter "X" by using equation (26) and replace ε with equation (27) in order to get equation (28).

For SDS solution (1 CMC), the parameter "X" is defined as:

$$\left(1+X^{2/3.61}\right)^{3.61}\left(\left(dp/dz\right)_{go}-\frac{\left(dp/dz\right)_{lo}}{X^2}\right)=9749\left(1-\frac{1}{\left(\left(1+0.0904X^{0.548}\right)^{2.82}\right)}\right) \qquad (29)$$

When the value of X is determined, ϕ_g is calculated from equation (26). The two-phase pressure gradient, $(dp/dz)_{tp}$ then can be calculated from equation (22).

We used the Lockhart-Martinelli model [9] to obtain the predicted pressure gradients, $(dp/dz)_{cal}$ and compared them with the measured pressure gradients, $(dp/dz)_{exp}$ in the annular and the mist flows. The single-phase pressure gradients were calculated with friction factors of, $f = 16/Re$ for $Re < 2000$ and $f = 0.0791 / (Re^{1/4})$ for $Re > 4000$.

Figure 4 shows the comparison between the measured $(dp/dz)_{exp}$ and the predicted $(dp/dz)_{cal}$ using equations (1) to (29). The predicted $(dp/dz)_{cal}$ values from the theory agree well with the measured $(dp/dz)_{exp}$ values. The measured $(dp/dz)_{exp}$ values of the pure water is closer to that of the theory than the SDS solution (1 CMC).

4.4.5 Effect of $Re_{SDS\ solution}$ at 1 CMC on the Bubble and Taylor Bubble Sizes

Figures 5(a) and 5(b) show photographs of the bubbles of pure water at $Re_{water} = 480$, $Re_{air} = 5.64$ vs. the bubbules of SDS solution (1 CMC) at $Re_{SDS} = 500$ and $Re_{air} = 5.64$. The presence of surfactants made the solution more opaque than that of pure water.

Figure 6(a) to 6(c) shows the bubble width, the bubble height and the equivalent diameter vs. air Reynolds number, Re_{air}. As we varied Re_{liquid}, the bubble width changed slightly, it varied between 14.4-18.4 mm for pure water, and 14.2-17.5 mm for the SDS solution (1 CMC). When we fixed Re_{liquid} but with increasing Re_{air}, the bubble width seemed to be constant for pure water but slightly increased for

the SDS solution (1 CMC). For the bubble height, as we varied Re_{liquid} it increased from 6.7 to 14 mm for pure water, and from 8.1 to 13.5 mm for the SDS solution (1 CMC). When we fixed Re_{liquid}, the bubble height increased sligthly with increasing Re_{air} for both of pure water and the SDS solution (1 CMC). The increasing rate of the bubble height for the SDS solution (1 CMC) was higher than that of pure water. We may note that $Re_{critical}$ values of the slug flow regime for SDS solution (1 CMC) shifted to the lower Re_{air} value than those of the pure water.

Figure 7(a) to 7(c) shows the effect of $Re_{SDS\ solution}$ on the length of the Taylor bubble. When we fixed Re_{liquid} with increasing Re_{air}, the length of Taylor bubble for pure water and the SDS solution (1 CMC) increased linearly with Re_{air}. At Re_{liquid} =0, the Taylor slug length was the same, smaller, and longer than that of pure water. This presumably arises because at same but low Re_{air}, the effect of SDS solution viscosity dominated to keep the slug length short. On the other hand, at high but the same Re_{air}, the effect of surface tension dominated. For Re_{liquid} ~ 1,000 and 2,500, the Taylor slug length of SDS solution was larger than that of pure water. At high Re_{liquid}, the effect of solution viscosity diminished and the lower surface tension produced longer Taylor slugs. We may note that the pressure gradient (dp/dz) of the SDS solution (1 CMC) was lower than that of pure water in both the slug and the slug-churn flow regimes.

4.4.6 Effect of $Re_{SDS\ solution}$ at 1 CMC on The Bubble Velocity

Figure 8 shows the bubble velocity for pure water and the SDS solution (1 CMC) vs. air Reynolds number, Re_{air}. We can see that as we fixed Re_{air}, the bubble velocity increased with increasing Re_{liquid}. When Re_{liquid} was fixed, the bubble velocity seemed to be independent of Re_{air} for both of pure water and the SDS solution (1 CMC). At the same liquid Reynolds number, the bubble velocity of the SDS solution (1 CMC) was higher than that of the bubble velocity of pure water. The last effect is a direct consequence of a lower surface tension.

4.5 Conclusions

The experiments were carried out on the two-phase upward flows consisting gas and liquid in a vertical tube with an inner diameter 0.019 m and 3 m in length for air-water and air-SDS solution (1 CMC) systems in order to investigate the influence of surfactant addition on the flow regimes, the corresponding pressure gradients, the bubble size and the bubble velocity.

The boundaries of the bubble, the bubble-slug and the slug flow regimes in SDS solution (1CMC) shifted to the left or smaller values relative to those of pure water. But the boundaries for the churn, the annular and the mist flow regimes remained nearly the same. In the bubble, the bubble-slug and the slug flows, the critical Reynolds numbers of air, $(Re_{air})_{critical}$ were relatively low and the flow was laminar. The effect of surface tension was more pronounced in these regimes. For the churn, the annular and the mist flows, the critical Reynolds numbers of air, $(Re_{air})_{critical}$ were relatively high and the flow was turbulent. So, the effect of viscosity and surface tension in these regimes were relatively less.

Fluctuations of pressure gradients, $(dp/dz)_{exp}$, were less sever in the SDS solution (1CMC) than those in pure water because of the viscosity effect. The highest fluctuations occurred in the slug and the slug-churn regimes of both pure water and the SDS solutions.

At the same liquid Reynolds numbers, the pressure gradients, $(dp/dz)_{exp}$, of the SDS solution (1 CMC) seemed to be equal to the pressure gradients, $(dp/dz)_{exp}$, of the pure water in the bubble and the bubble-slug flow regimes. The pressure gradients, $(dp/dz)_{exp}$, of the SDS solution (1 CMC) were lower than the pressure gradients, $(dp/dz)_{exp}$, of the pure water in the slug to the slug-churn regime because the flows were turbulent and the effect of surface tension was more pronounced in these regimes. The pressure gradients were nearly equal to each other again from the churn flow to the mist flow regime because Re_{air} were high and the flows were turbulent.

At same Re_{liquid}, the pressure gradients, $(dp/dz)_{exp}$, of the SDS solution at 0.5, 1 and 2 CMC were nearly equal to each others but lower than the pressure gradient (dp/dz) of pure water from the slug to the slug-churn flow regimes because

the surface tension and viscosity of all SDS solutions were nearly equal to each other. The pressure gradients of water and the SDS solution became equal to each other again in the churn flow regime because Re_{air} were high and flow was turbulent.

The proposed theories for the pressure gradient by Nicklin, Wilkes, and Davidson (1962) for the bubble and the slug flow regimes, Sylvester (1987) for the slug flow regime and by Wallis (1969) for the annular and the mist flow regimes are in moderately good agreement with the measured values.

When we fixed Re_{liquid} with increasing Re_{air}, the bubble width seemed to be constant for pure water but slightly increased for SDS solution (1 CMC). At low Re_{air}, the bubble height of the SDS solution was lower than those of pure water because of the viscosity played more pronounced role than that the surface tension. But at higher Re_{air}, the bubble height of SDS solution was higher than those of pure water because of the surface tension played a more pronounced role than that of the viscosity. The increasing rate of the bubble height for the SDS solution (1 CMC) was higher than that of pure water because of the surface tension effect. As fixed Re_{liquid} with increasing Re_{air}, the length of Taylor bubble for the SDS solution (1 CMC) was longer than pure water because of surface tension effect. The pressure gradient (dp/dz) for the SDS solution (1 CMC) was lower than that of pure water in the slug and the slug-churn flow regime.

As we fixed Re_{air}, the bubble velocity increased with increasing Re_{liquid}. At the same liquid Reynolds number, the bubble velocity of SDS solution (1 CMC) was higher than the bubble velocity of pure water because of the surface tension effect.

4.6 Acknowledgements

This work was supported by Postgraduate Education and Research Programs in Petroleum and Petrochemical Technology (PPT Consortium under ADB fund), Chulalongkorn University.

4.7 References

[1] J.O. Wilkes, Fluid Mechanics for Chemical Engineers, Prentice-Hall PTR, New Jersey, 1999.

[2] D.J. Nicklins, J.O. Wilkes, J.F. Davidson, Two-phase Flow in Vertical Tubes, Transactions of the Institute of Chemical Engineers 40 (3) (1962) 61-68.

[3] H. Cheng, J.H. Hills, B.J. Azzorpardi, A Study of the Bubble-to-Slug Transition in Vertical Gas–Liquid Flow in Columns of Different Diameter, International Journal of Multiphase flow 24(3) (1998) 431-452.

[4] T.R. Nigmatulin, F.J. Bonetto, Shape of Taylor Bubbles in Vertical Tubes, International Communication of Heat and Mass Transfer 24(8) (1997) 1177-1185.

[5] X.T. Chen, J.P. Brill, Slug to Churn Transition in Upward Vertical Two-Phase Flow, Chemical Engineering Science 52(23) (1998) 4269-4272.

[6] G.W. Govier, K. Aziz, The Flow of Complex Mixtures in Pipes, Van Nostrand Reinhold, New York, 1972.

[7] R.M. Davies, G.I. Taylor, The Mechanics of Large Bubbles Rising Through Extended Liquids and Through Liquids in Tubes, Proceedings of Royal. Society. 200A (1950) 375-390.

[8] G.B. Walllis, One-dimensional Two-phase Flow, McGraw Hill, New York, 1969.

[9] R.W. Lockhart, R.C. Martinelli, Proposed Correlation of Data for Isothermal Two-phase, Two-component Flow in Pipes, Chemical Engineering Progress 45(1) (1949) 39-48.

[10] N.D. Sylvester, A Mechanistic Model for Two-Phase Vertical Slug Flow in Pipes, Journal of Energy Resources Technology, Transactions of the ASME 109(4) (1987) 206-213.

[11] T. Furakawa, T. Fukano, Effect of Liquid Viscosity on Flow Patterns in Vertical Upward Gas-Liquid Two-Phase Flow, International Journal of Multiphase Flow 27(1) (2001) 1109-1126.

[12] D.A. McNeil, A.D. Stuart, The Effects of Highly Viscous Liquid Phase on Vertically Upward Two-Phase Flow in a Pipe, International Journal of Multiphase Flow 29 (2003) 1523-1549.

[13] M. Dziubinski, H. Fidos, M. Sosno, The Flow Pattern Map of a Two-Phase non-Newtonian Liquid-Gas Flow in Vertical Pipe, International Journal of Multiphase Flow 30(1) (2004) 551-563.

[14] M.R, Malayeri, H. Muller-Steinhagen, J.M. Smith, Neural Network Analysis of Void Fraction in Air/Water Two-Phase Flows at Elevated Temperature, Chemical Engineering and Processing 42(1) (2003) 587-597.

[15] R.C. Fernandes, Experimental and Theoretical Studies of Isothermal Upward Gas-Liquid Flows in Vertical Tubes, Ph.D. thesis, University of Houston (1981).

[16] D. Zigrang, N.D. Sylvester, Explicit Approximation to the Solution of Colebook's Friction Factor Equation, AIChE Journal 28 (1982) 514.

[17] C. Aladjem Talvy, L. Shemer, D. Barnea, On the Interaction Between Two Consecutive Elongated Bubbles in a Vertical Pipe, International Journal of Multiphase Flow 26(1) (2000) 1905-1923.

[18] J.R. Barbosa Jr, G.F. Hewitt, G. Konig, S.M. Richardson, Liquid Entrainment, Droplet Concentration and Pressure Gradient at the Onset of Annular Flow in a Vertical Pipe, International Journal of Multiphase flow 28 (2002) 943-961.

[19] G. Costigan, P.B. Whalley, Slug Flow Regime Identification From Dynamic Void Fraction Measurements in Vertical Air-Water Flows, International Journal of Multiphase flow 23(2) (1997) 263-282.

[20] F. Farshad, H. Rieke, J. Garber, New Developments in Surface Roughness Measurements, Characterization, and Modeling Fluid Flow in Pipe, Journal of Petroleum Science and Engineering 29(1) (2001) 139-150.

[21] M. Kawaji, J.M. DeJesus, G. Tudose, Investigation of Flow Structure in Vertical Slug Flow, Nuclear Engineering and Design 175(1) (1997) 37-48.

[22] I. Kliakhandler, Fun with Bubble, The News and Information Publication of The society of Rheology 74(1) (2005) 6-7.

[23] D. Luo, M. Ghiaasiaan, Interphase Mass Transfer in Cocurrent Vertical Two-Phase Channel Flows with non-Newtonian Liquid, International Communication of Heat and Mass Transfer 24(1) (1997) 1-10.

[24] R. Luo, X.H. Pan, X.Y. Yang, Laminar Light Particle and Liquid Two-Phase Flows in a Vertical Pipe, International Journal of Multiphase Flow 29(1) (2003) 603- 620.

[25] K. Mishima, T. Hibiki, Some Characteristics of Air-Water Two-Phase Flow in Small Diameter Vertical Tubes, International Journal of Multiphase Flow 22(4) (1996) 703-712.

[26] T. Okawa, A. Kotani, I. Kataoka, Experiment for Liquid Phase Mass Transfer Rate in Annular Regime for a Small Vertical Tube, International Journal of Heat and Mass Transfer 48(1) (2005) 585-598.

[27] H.M. Prasser, E. Krepper, D. Lucas, Evolution of The Two-Phase Flow in a Vertical Tube-Decomposition of Gas Fraction Profiles According to Bubble Size Classes using Wire-Mesh Sensors, International Journal of Thermal Science 41(1) (2002) 17-28.

[28] P. Satitchaicharoen, S. Wongwises, Two-Phase Flow Pattern Maps for Vertical Upward Gas-Liquid Flow in Mini Gap Channels, International Journal of Multiphase Flow 30(1) (2004) 225-236.

[29] X. Shen, K. Mishima, H. Nakaymura,(2005) Two-Phase Phase Distribution in a Vertical Large Diameter Pipe, International Journal of Heat and Mass Transfer 48(1) (2005) 211-225.

[30] Q. Song, R. Luo, X.Y. Yang, Z. Wang, Phase Distributions for Upward Laminar Dilute Bubbly Flows with Non-Uniform Bubble Sizes in a Vertical Pipe, International Journal of Multiphase flow 27(1) (2001) 379-390.

[31] X. Sun, R. Smith, M.Y. Ishii, J. Uhle, Interfacial Area of Bubbly Flow in a Relative Large Diameter Pipe, Experimental Thermal and Fluid Science 27(1) (2002) 97-109.

[32] C. Wang, I.Y. Chen, P.S. Huang, Two-Phase Slug Flow Across Small Diameter Tubes with The Presence of Vertical Return Bend, International Journal of Heat and Mass Transfer 48(1) (2005) 2342-2346.

[33] A. Wolf, S. Jayanti, G.F. Hewitt, Flow Development in Vertical Annular Flow, Chemical Engineer Science 56 (2001) 3221-3235.

[34] S. Wongwises, W. Kongkiatwanitch, Interfacial Friction Factor in Vertical Upward Gas-Liquid Annular Two-Phase Flow, International Journal of Heat and Mass Transfer 28(3) (2001) 323-336.

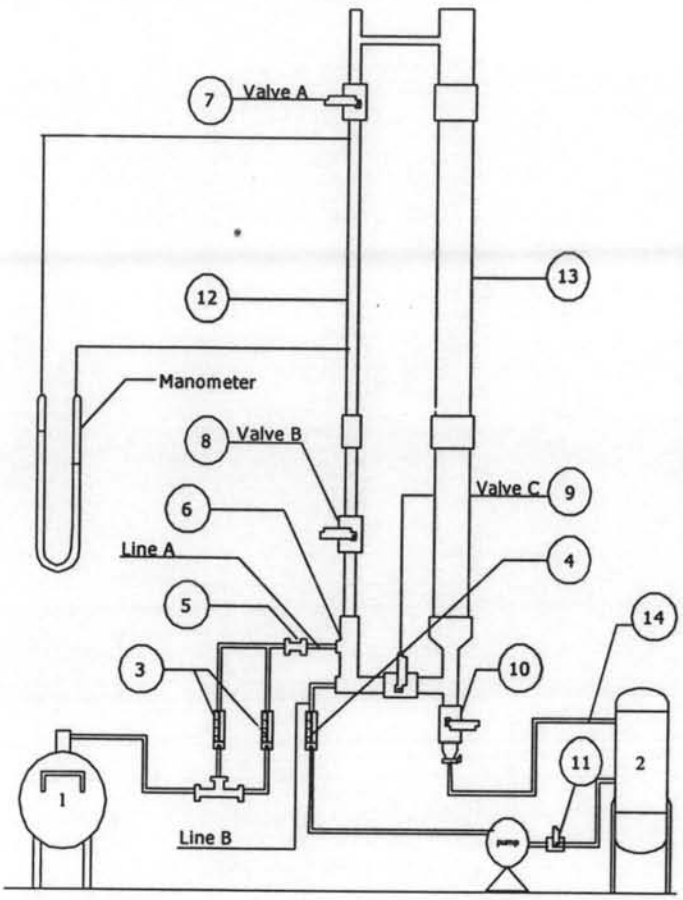

1. Air compressor maximum 10 bar
2. Solution reservoir tank
3. Air rotameter
4. liquid rotameter
5. check value
6. Air injection tee
7. Ball valve A
8. Ball valve B
9. Ball valve C
10. Draining ball valve
11. Control valve for reservoir tank
12. Acrylic tube (1.9 cm)
13. Overflow acrylic tube (5.4 cm)
14. Solution return line to reservoir

Line A Air injection line
Line B Solution injection line

Figure 1 Schematic diagram of the experimental set up.

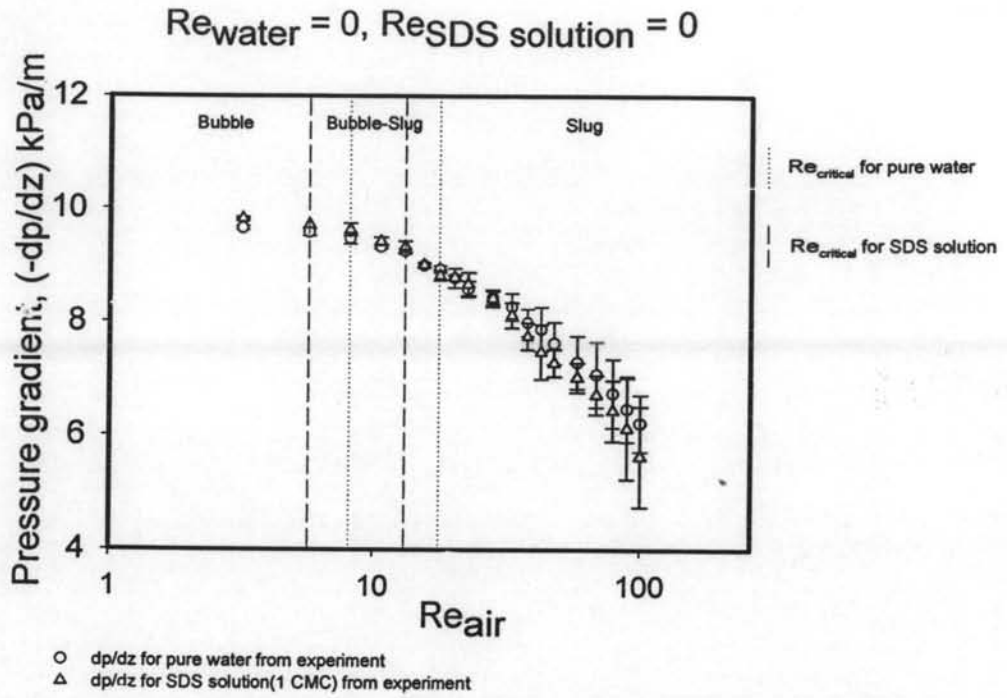
Re water = 0, Re SDS solution = 0
Pressure gradient, (-dp/dz) kPa/m
12
10
8
6
4
Bubble
Bubble-Slug
Slug
Re critical for pure water
Re critical for SDS solution
1
10
100
Re air
dp/dz for pure water from experiment
dp/dz for SDS solution(1 CMC) from experiment

(a)

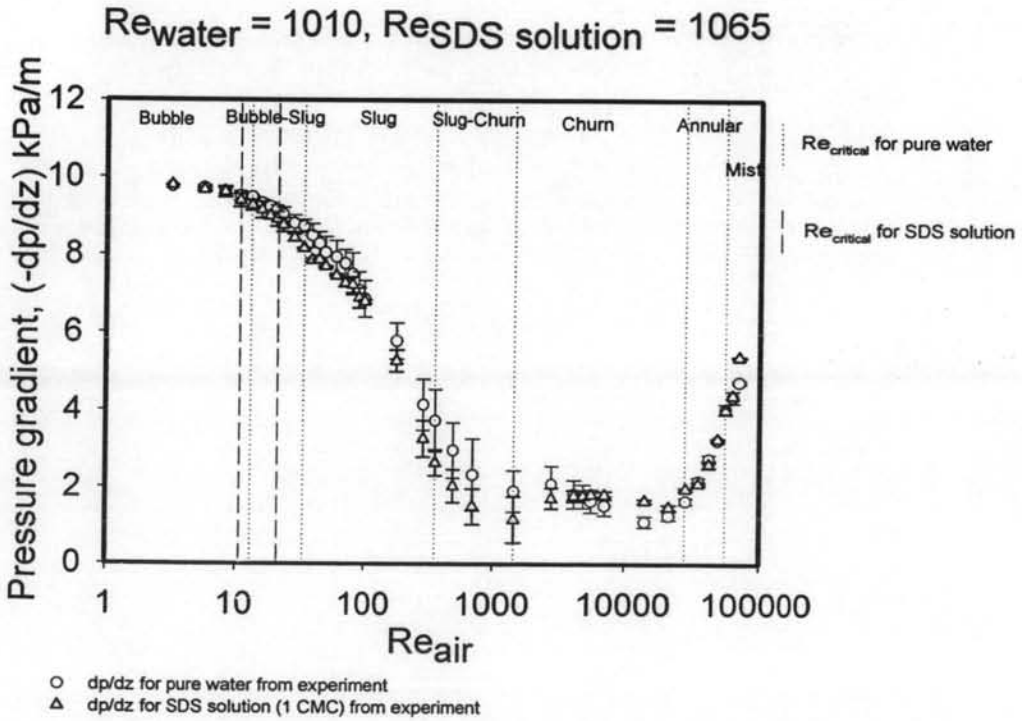
Re water = 1010, Re SDS solution = 1065
Pressure gradient, (-dp/dz) kPa/m
12
10
8
6
4
2
0
Bubble
Bubble-Slug
Slug
Slug-Churn
Churn
Annular
Mist
Re critical for pure water
Re critical for SDS solution
1
10
100
1000
10000
100000
Re air
dp/dz for pure water from experiment
dp/dz for SDS solution (1 CMC) from experiment

(b)

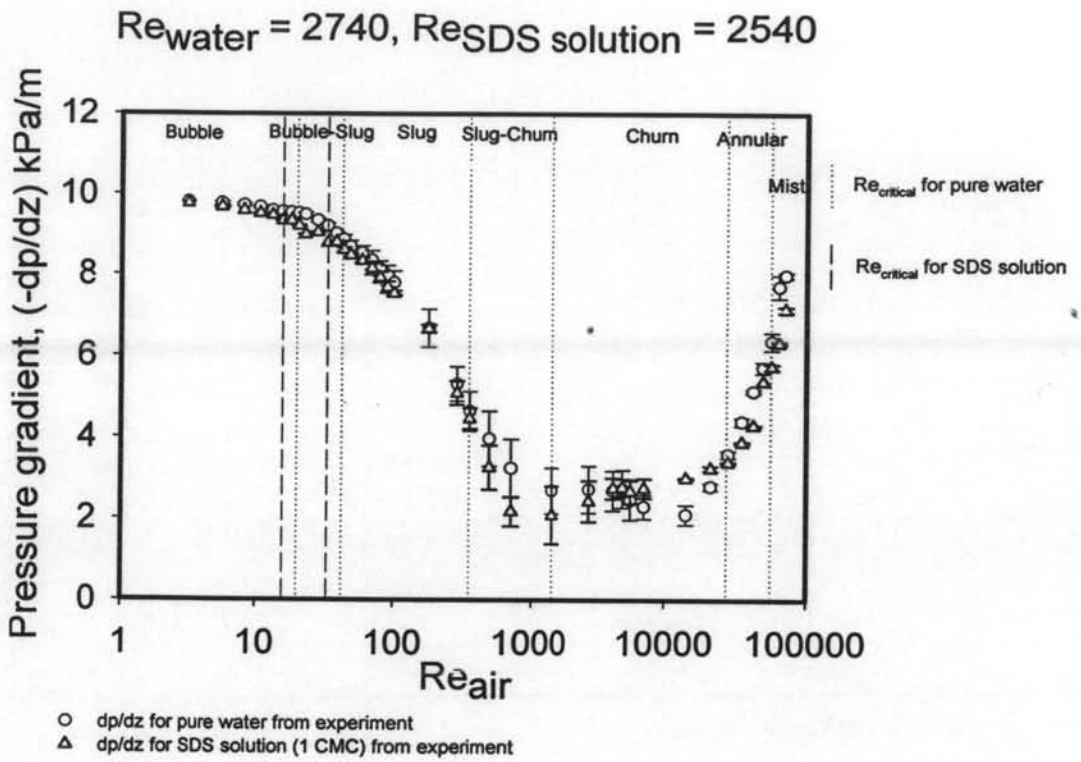

(c)

Figure 2 Effect of $Re_{SDS\ solution}$ on pressure gradient (dp/dz): a) $Re_{water} = 0$ and $Re_{SDS\ solution} = 0$; b) $Re_{water} = 1010$ and $Re_{SDS\ solution} = 1065$; c) $Re_{water} = 2740$ and $Re_{SDS\ solution} = 2540$.

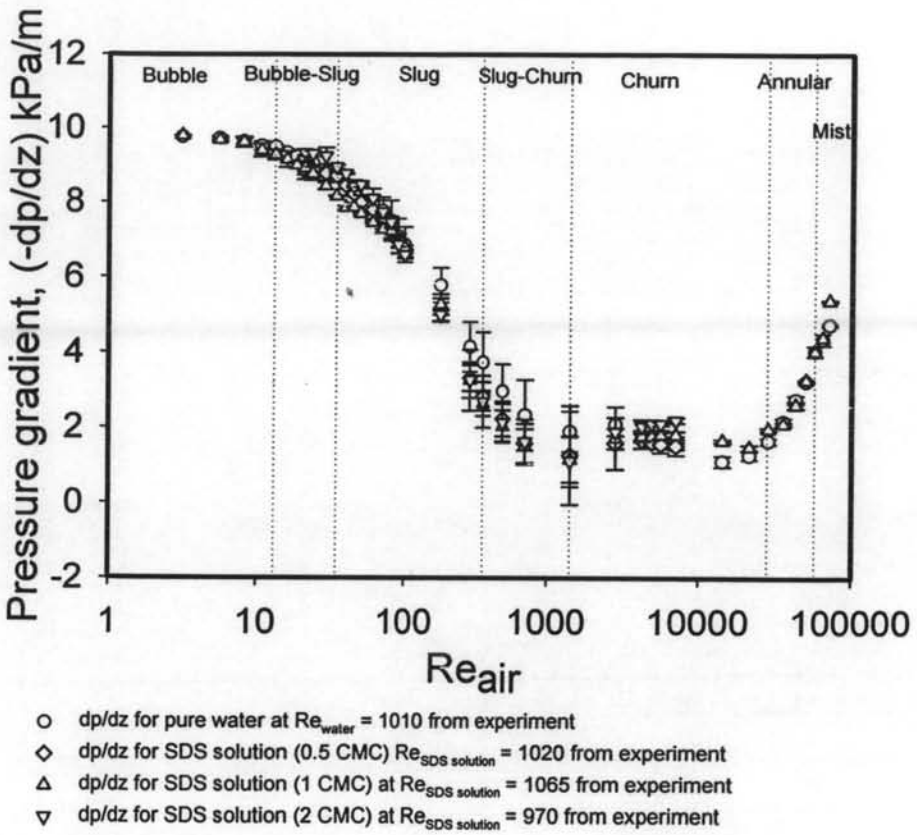

Figure 3 Effect of surfactant concentration on pressure gradient (dp/dz).

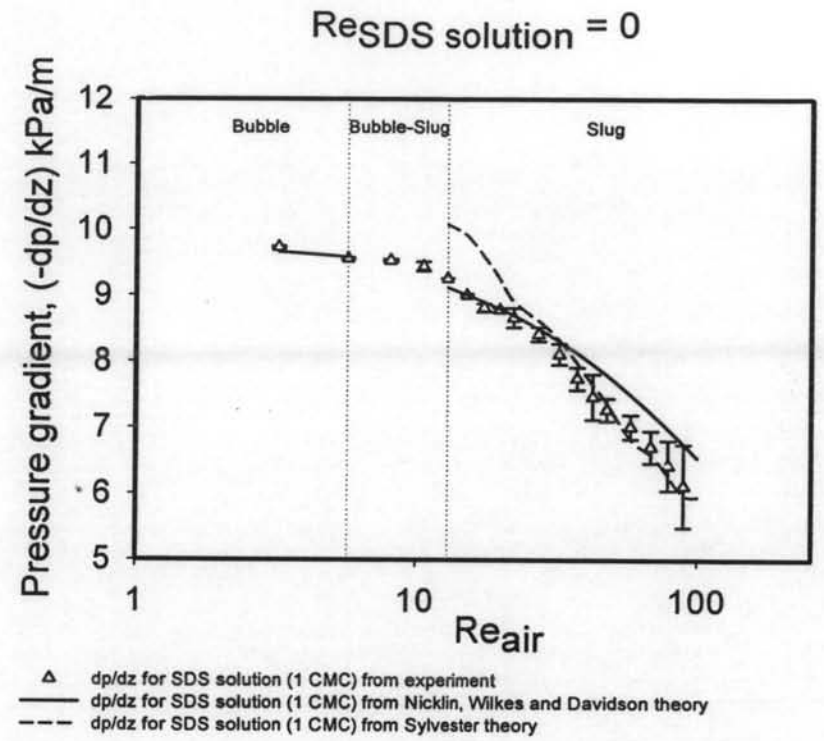
Re SDS solution = 0
Pressure gradient, (-dp/dz) kPa/m
12
11
10
9
8
7
6
5
Bubble
Bubble-Slug
Slug
1
10
100
Re air
dp/dz for SDS solution (1 CMC) from experiment
dp/dz for SDS solution (1 CMC) from Nicklin, Wilkes and Davidson theory
dp/dz for SDS solution (1 CMC) from Sylvester theory

(a)

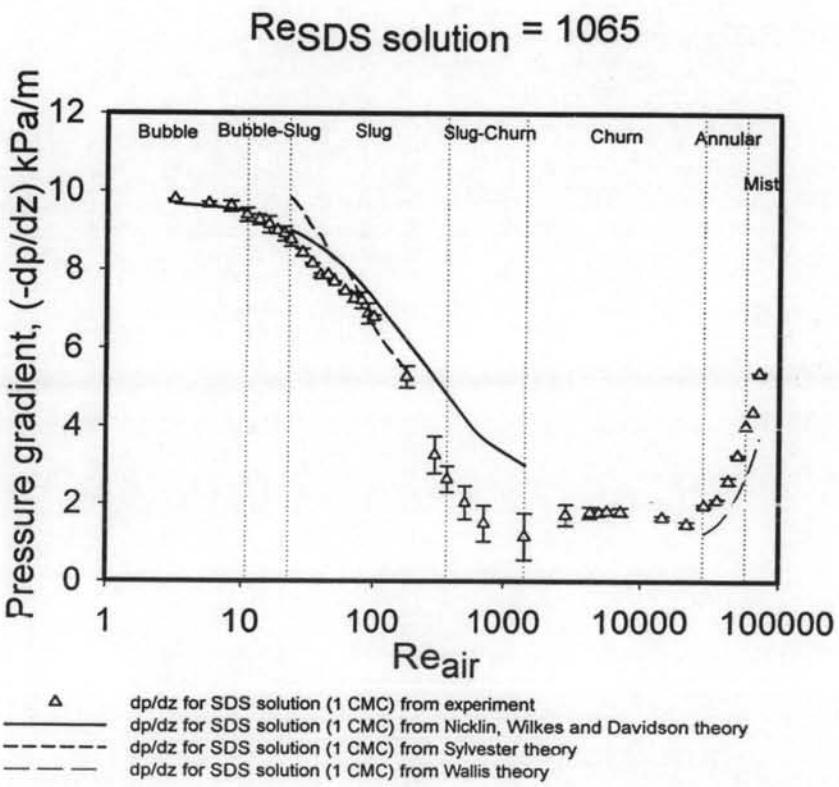
Re SDS solution = 1065
Pressure gradient, (-dp/dz) kPa/m
12
10
8
6
4
2
0
Bubble
Bubble-Slug
Slug
Slug-Churn
Churn
Annular
Mist
1
10
100
1000
10000
100000
Re air
dp/dz for SDS solution (1 CMC) from experiment
dp/dz for SDS solution (1 CMC) from Nicklin, Wilkes and Davidson theory
dp/dz for SDS solution (1 CMC) from Sylvester theory
dp/dz for SDS solution (1 CMC) from Wallis theory

(b)

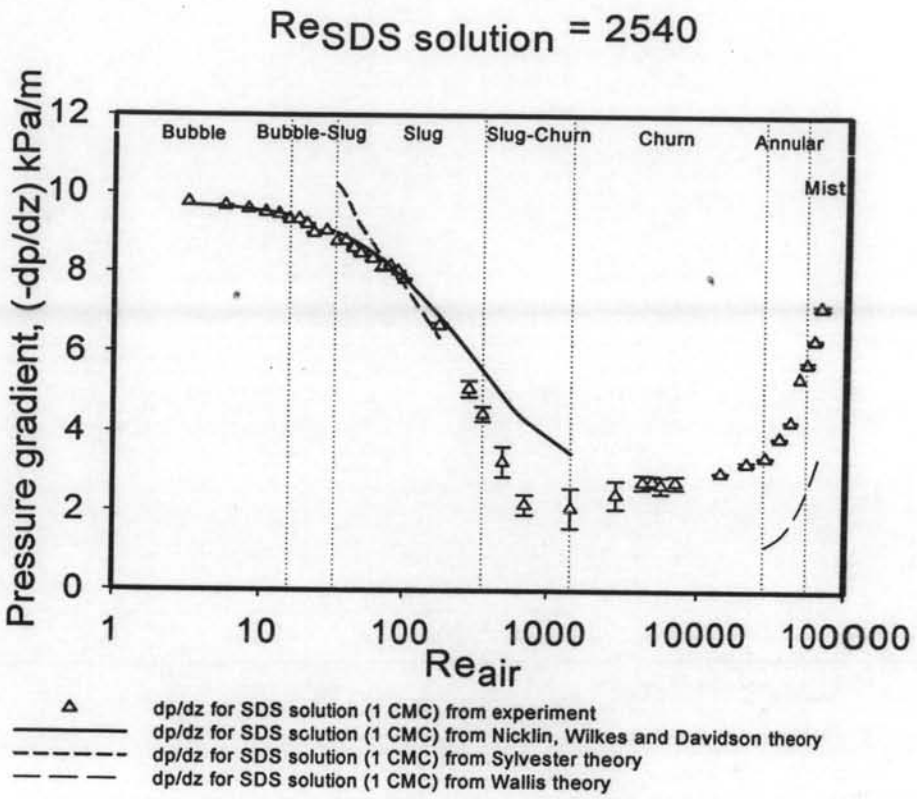

(c)

Figure 4 Comparison between theoretical and measured pressure gradients, (dp/dz): a) $Re_{SDS\ solution} = 0$; b) $Re_{SDS\ solution} = 1065$; c) $Re_{SDS\ solution} = 2540$.

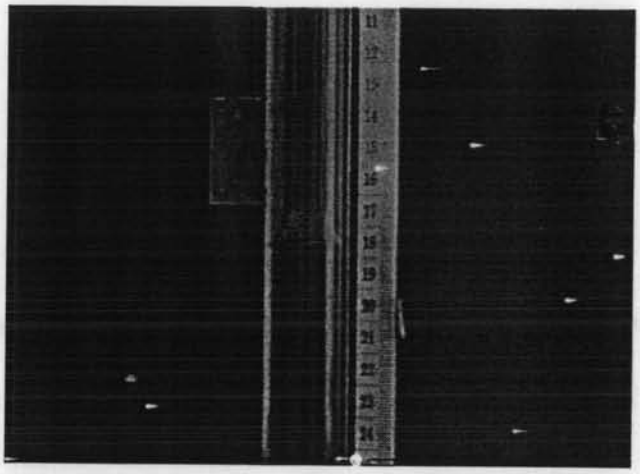

(a)

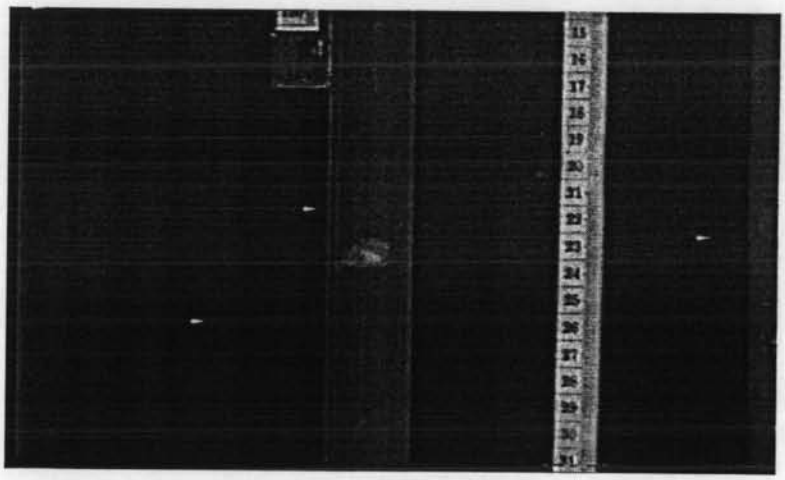

(b)

Figure 5 Photograph of the bubble flow regime: a) pure water at Re_{water} = 480, Re_{air} = 5.64; b) SDS solution (1 CMC) at Re_{SDS} solution at 1 CMC = 500, Re_{air} = 5.64.

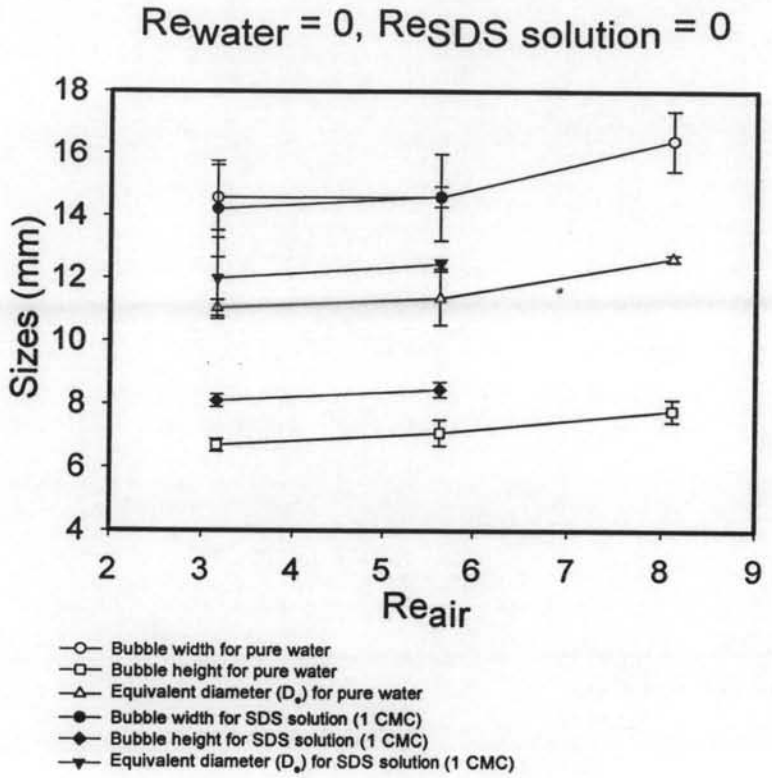
Re water = 0, Re SDS solution = 0
Sizes (mm)
Re air
Bubble width for pure water
Bubble height for pure water
Equivalent diameter (De) for pure water
Bubble width for SDS solution (1 CMC)
Bubble height for SDS solution (1 CMC)
Equivalent diameter (De) for SDS solution (1 CMC)

(a)

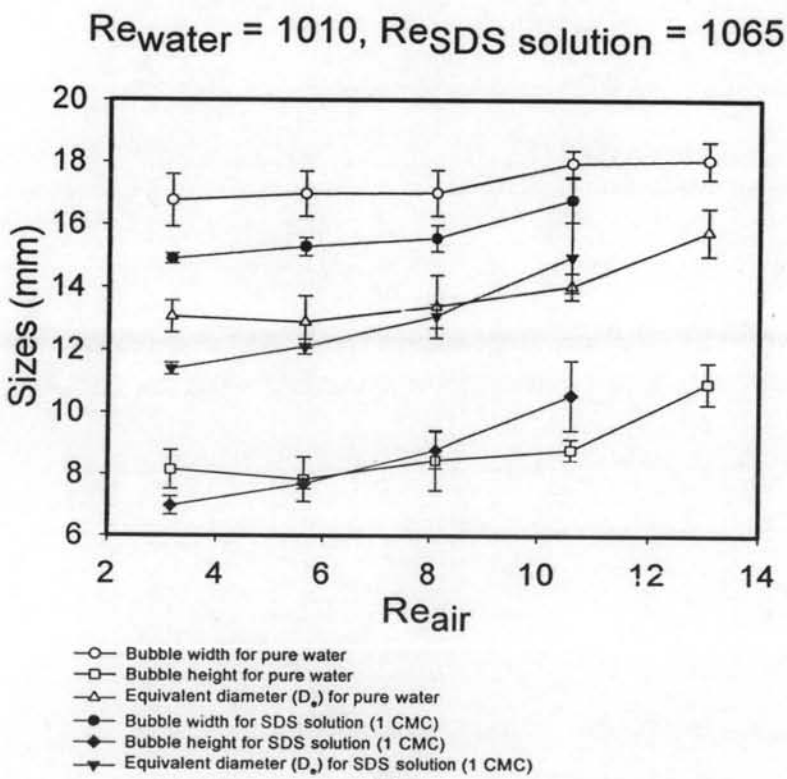
Re water = 1010, Re SDS solution = 1065
Sizes (mm)
Re air
Bubble width for pure water
Bubble height for pure water
Equivalent diameter (De) for pure water
Bubble width for SDS solution (1 CMC)
Bubble height for SDS solution (1 CMC)
Equivalent diameter (De) for SDS solution (1 CMC)

(b)

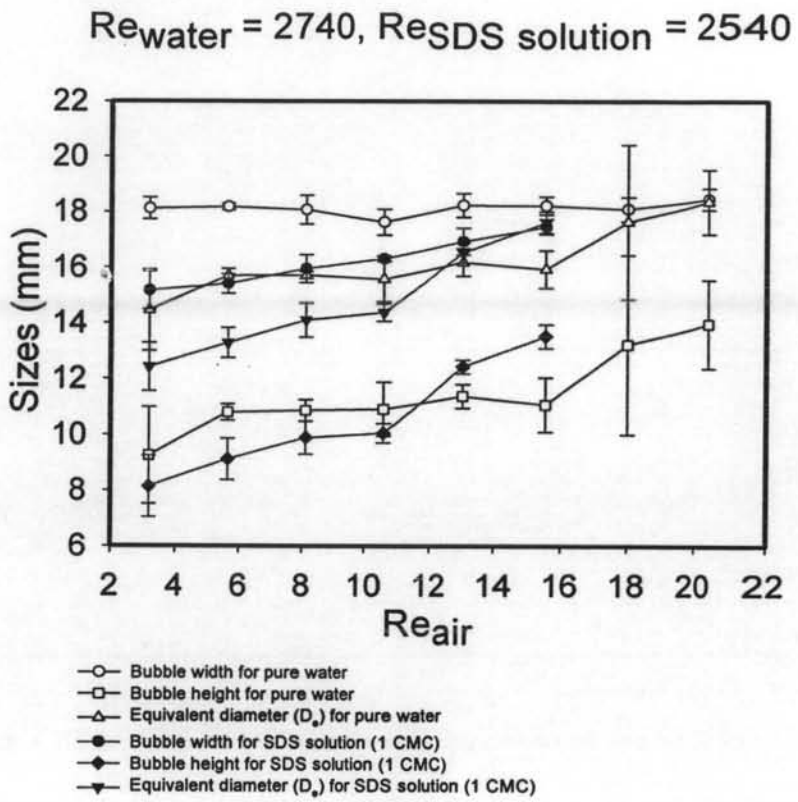

(c)

Figure 6 Effect of $Re_{SDS\ solution}$ on the bubble size: a) $Re_{water} = 0$ and $Re_{SDS\ solution} = 0$; b) $Re_{water} = 1010$ and $Re_{SDS\ solution} = 1065$; c) $Re_{water} = 2740$ and $Re_{SDS\ solution} = 2540$.

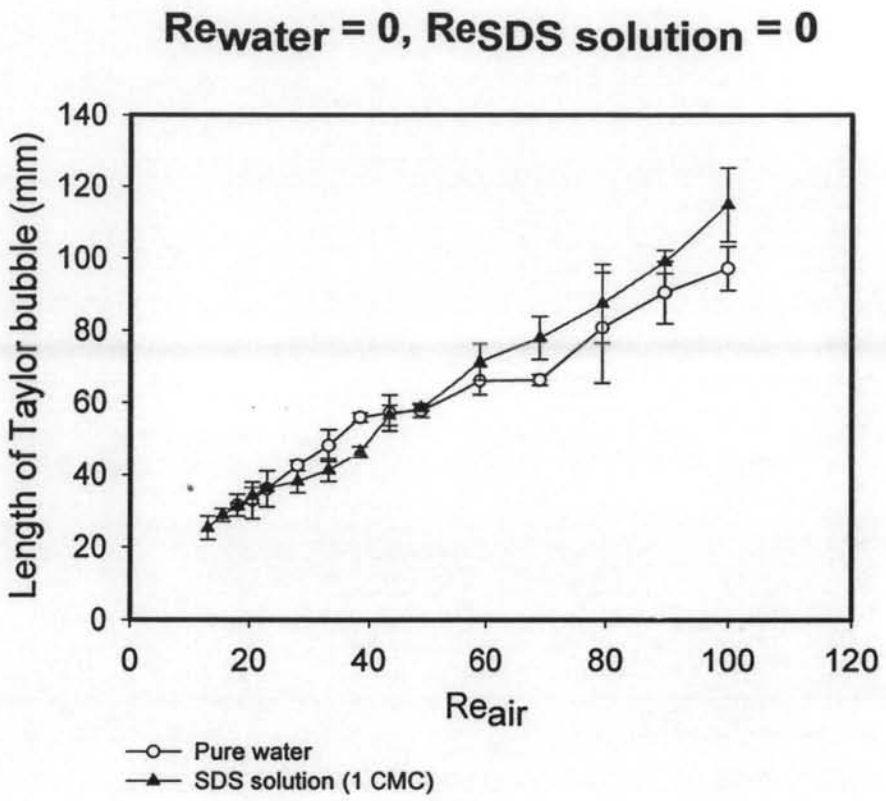
Rewater = 0, ReSDS solution = 0
Length of Taylor bubble (mm)
0
20
40
60
80
100
120
140
Reair
Pure water
SDS solution (1 CMC)

(a)

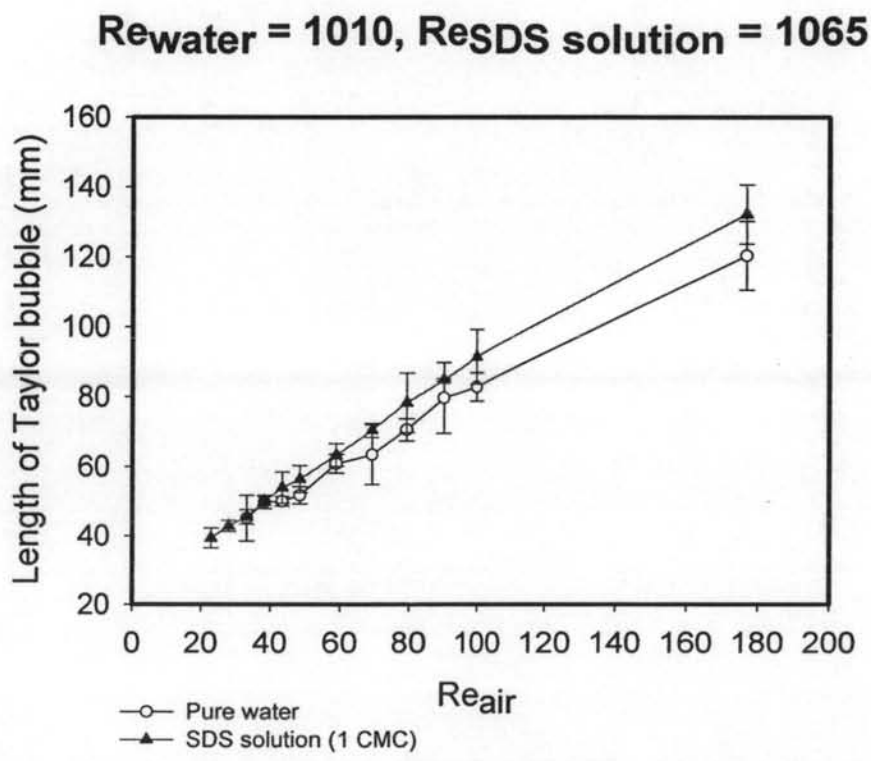
Rewater = 1010, ReSDS solution = 1065
Length of Taylor bubble (mm)
20
40
60
80
100
120
140
160
180
200
Reair
Pure water
SDS solution (1 CMC)

(b)

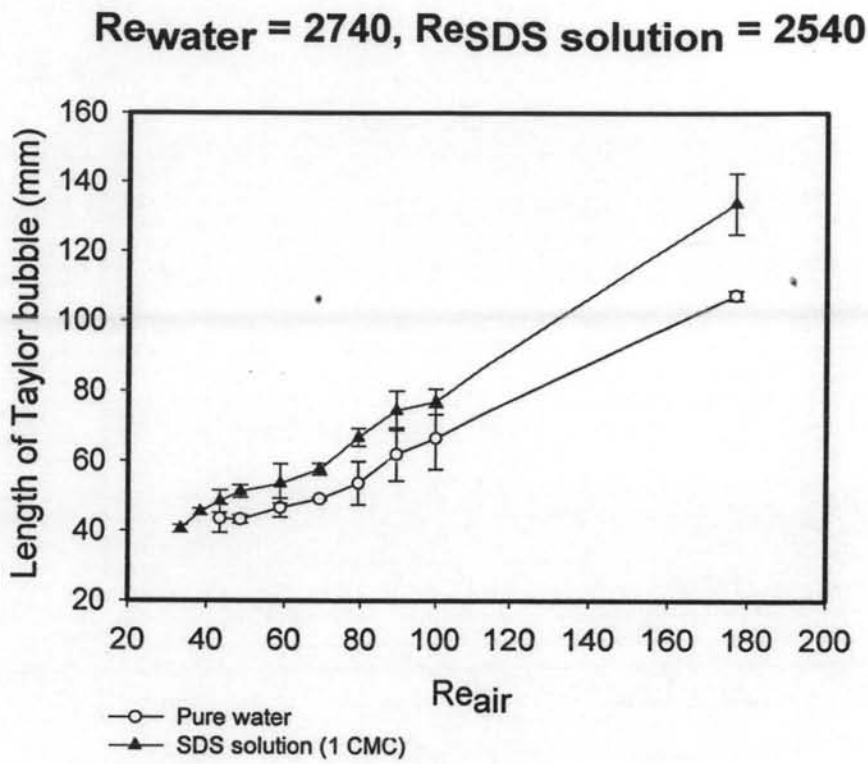

(c)

Figure 7 Effect of $Re_{SDS\ solution}$ on the length of Taylor bubble: a) Re_{water} = 0 and $Re_{SDS\ solution}$ = 0; b) Re_{water} = 1010 and $Re_{SDS\ solution}$ = 1065; c) Re_{water} = 2740 and $Re_{SDS\ solution}$ = 2540.

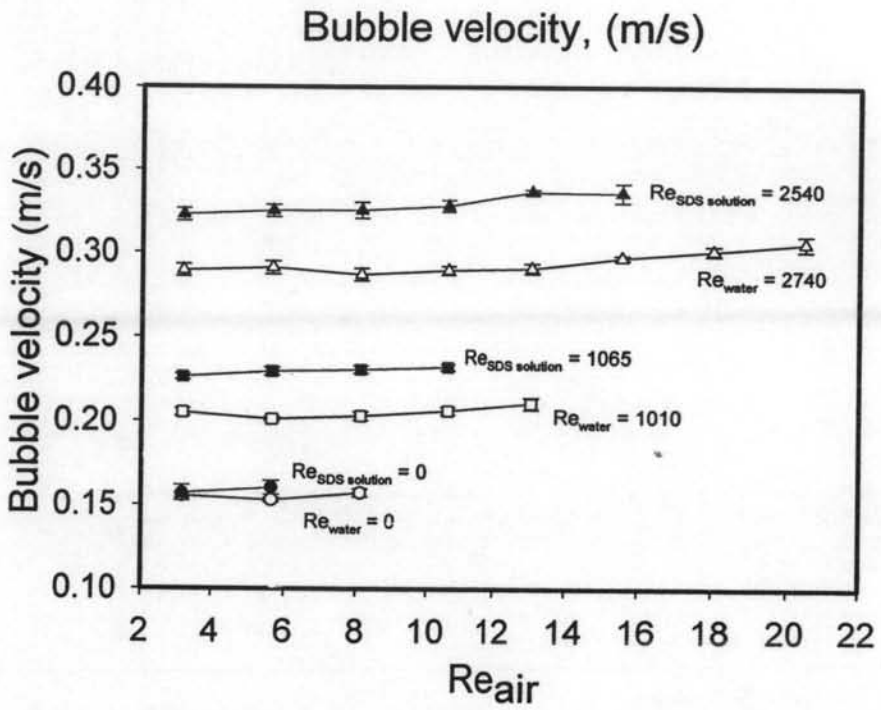

Figure 8 Effect of $Re_{SDS\ solution}$ on the bubble velocity.

Table 1 Physical properties of liquids used in the experiment

Liquid	ν_L (m^2/s)	μ (Pa.s)	ρ_L (kg/m^3)	σ ($\mu S/cm$)	Γ (mN/m)
Water	0.85×10^{-6}	8.48×10^{-4}	994.7	1.7	71.27
SDS solution (0.5 CMC)	9.34×10^{-7}	9.3×10^{-4}	994.8	1016	22.02
SDS solution (1 CMC)	1.02×10^{-6}	1.01×10^{-3}	994.97	1939	21.81
SDS solution (2 CMC)	1.09×10^{-6}	1.09×10^{-3}	995.58	2692	21.6

ν_L: kinematic viscosity, μ: viscosity , ρ_L: density, σ: electrical conductivity, and Γ: surface tension

System temperature, $T = 31^{\circ}C$ ($\pm 1^{\circ}C$)

1 CMC = 2.75 g/L

Table 2 The critical Reynolds numbers $(Re_{air})_{critical}$ of various regimes

Liquid	$Re_{air(critical)}$ for each flow regime						
	Re_{liquid}	Bubble-slug	Slug	Slug-churn	Churn	Annular	Mist
Water	0	10.6	18	-	-	-	-
SDS solution (1 CMC)	0	8.1	13.1	-	-	-	-
Water	1010	15.5	33.2	356	2850	28500	57000
SDS solution (0.5 CMC)	1070	13.1	20.5	356	2850	28500	57000
SDS solution (1 CMC)	1020	13.1	20.5	356	2850	28500	57000
SDS solution (2 CMC)	970	13.1	20.5	356	2850	28500	57000
Water	2740	23	43.5	356	2850	28500	57000
SDS solution (1 CMC)	2540	18	33.2	356	2850	28500	57000